

Figure S1 (related to Figure 1). Stimulated Emission Depletion (STED) Super Resolution Image of Striatal RanGAP1 in the R6/2 Mouse Model of HD. Severe intranuclear aggregation of RanGAP1 (red) in the striatum of 10 week old TG R6/2 mice.

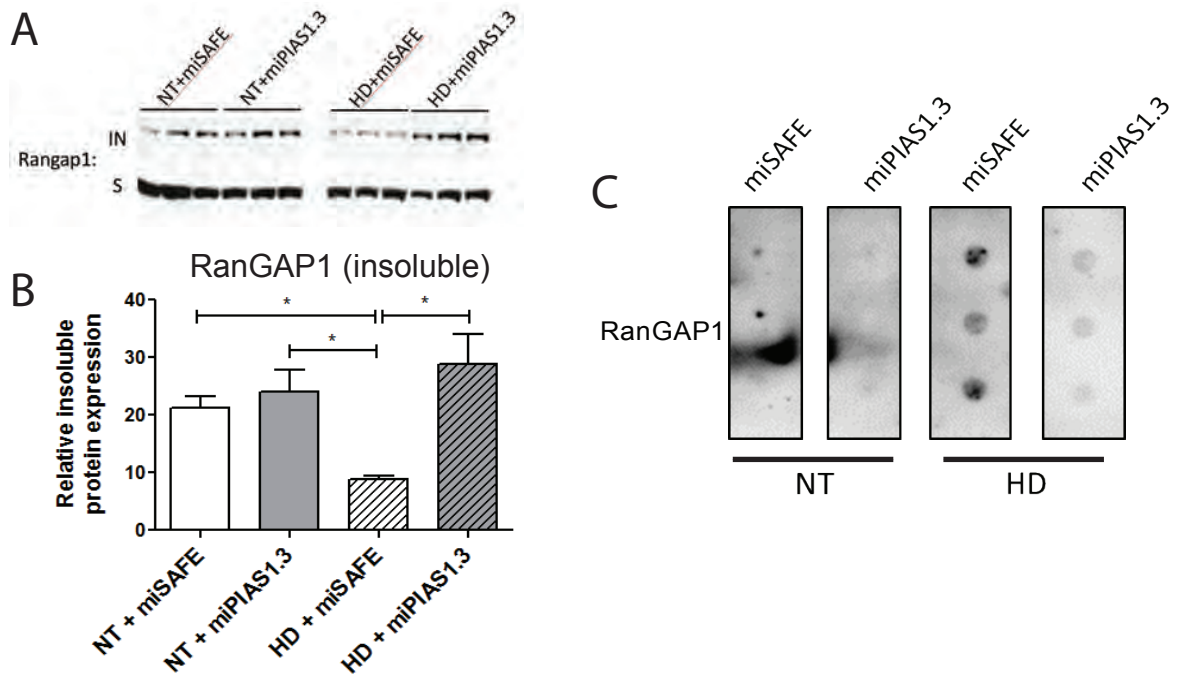


Figure S2 (related to Figure 1). Immunoblotting of RanGAP1 from 10-Week-Old R6/2 and Non-Transgenic Mouse Striatal Lysates Following Viral Mediated miSAFE or miPIAS1.3 Treatment. (A) Insoluble RanGAP1 levels are significantly reduced in the striatum of R6/2 mice compared to non-transgenic (NT) mice. Following miPIAS1.3 treatment, insoluble RanGAP1 levels are significantly increased in R6/2, but not NT mice compared to miSAFE treatment. (B) All data are expressed as western densitometry quantitation. Protein expression was validated for protein loading prior to antibody incubation using reversible protein stain and each samples' corresponding soluble α -tubulin expression. (C) Insoluble RanGAP1 accumulates and is sequestered into insoluble fibular aggregates in the striatum of R6/2 mice compared to NT mice as measured by filter retardation assay. Following miPIAS1.3 treatment, accumulated insoluble RanGAP1 is reduced relative to miSAFE treated R6/2 mice. Quantified data are presented as mean \pm SEM. * $P < 0.05$ as analyzed by two-way ANOVA followed by Tukey's post-hoc analysis.

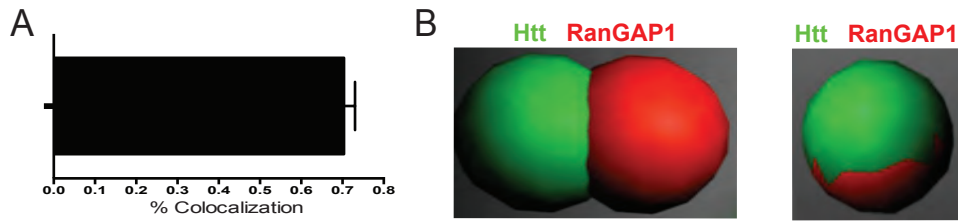


Figure S3 (related to Figure 2). Colocalization of Striatal RanGAP1 and mHtt Aggregates in the zQ175 Mouse Model of HD. IMARIS imaging software was employed to analyze colocalization of RanGAP1 and mHtt following immunostaining and confocal imaging. Approximately 70% of RanGAP1 aggregates were found to colocalize with mHtt aggregates in striatal and cortical neurons.

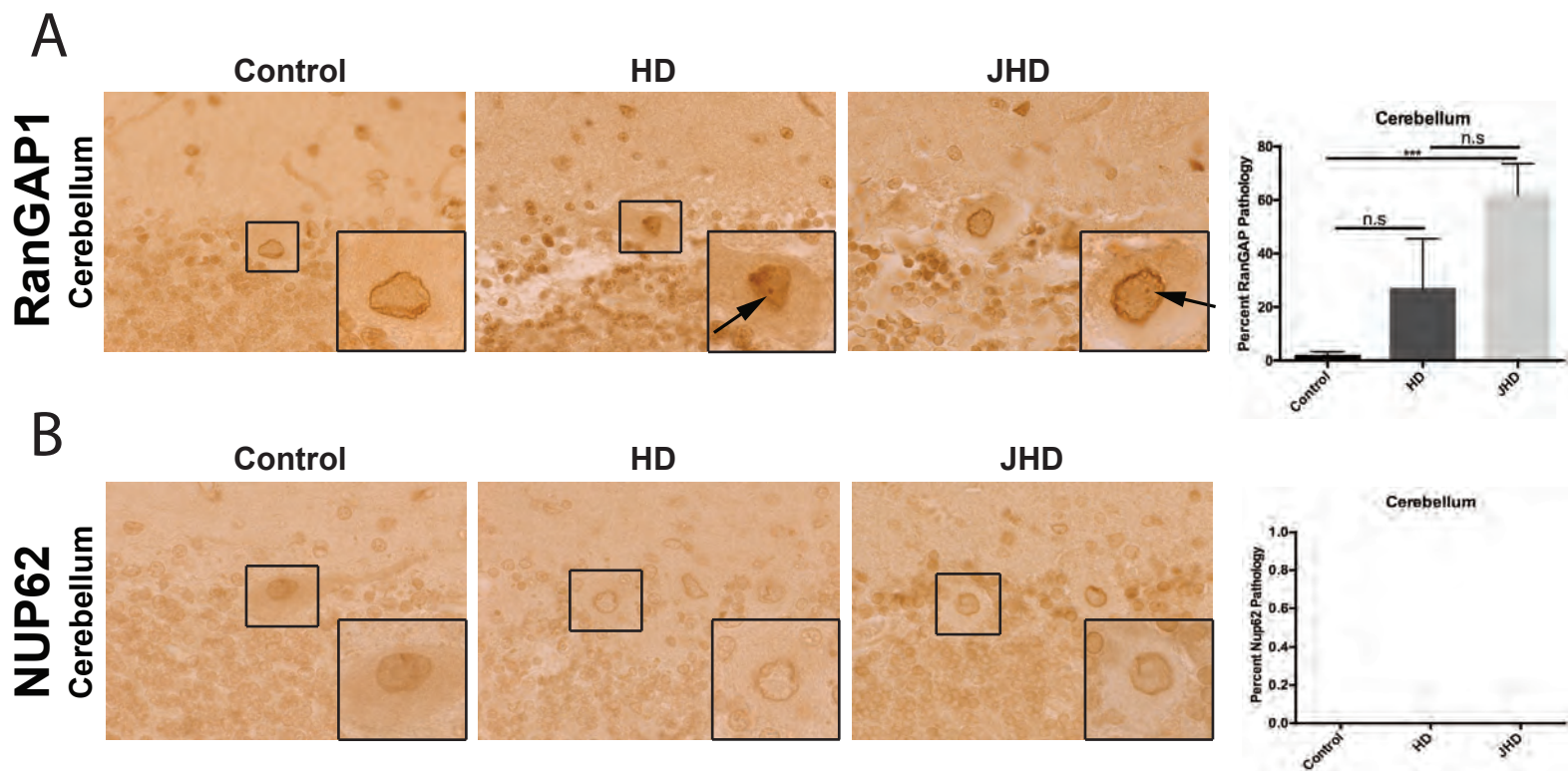


Figure S4 (related to Figure 3). RanGAP1 and NUP62 Immunostaining in Human HD and JHD Cerebellum. (A) RanGAP1 immunostaining in non-neurological disease control (n=10), HD (n=5), and JHD (n=5) cerebellum showing aggregates of RanGAP1 (arrows). Quantitation of percent of RanGAP1-positive cells with RanGAP1 pathology (aggregation) shown on the right of the representative images. Data are presented as mean \pm SEM. *** $P < 0.001$ as analyzed by one-way ANOVA followed by Tukey's post-hoc analysis. (B) NUP62 immunostaining in non-neurological disease control (n=10), HD (n=5), and JHD (n=5) cerebellum showing no pathology. Quantitation of percent of NUP62-positive cells with NUP62 pathology shown on the right of the representative images. Data are presented as mean \pm SEM

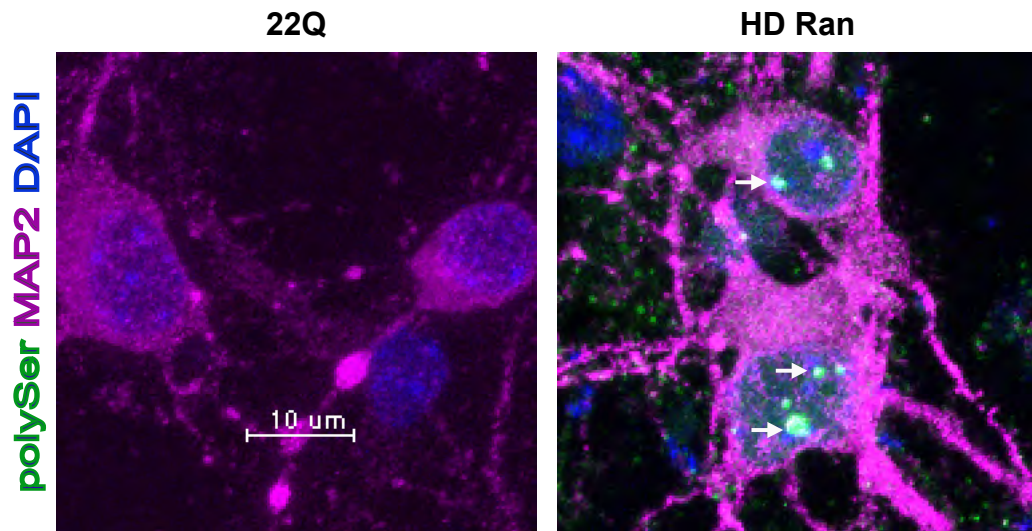


Figure S5 (related to Figure 6). Detection of HD-RAN Protein After Transfection with 6xStop-(CAG)80. Detection of polySer HD-RAN protein aggregates (arrows) after transfection with 6xStop-(CAG)80 in primary cortical neurons. PolySer HD-RAN protein aggregates are not detected after transfection with HTT 22Q control.

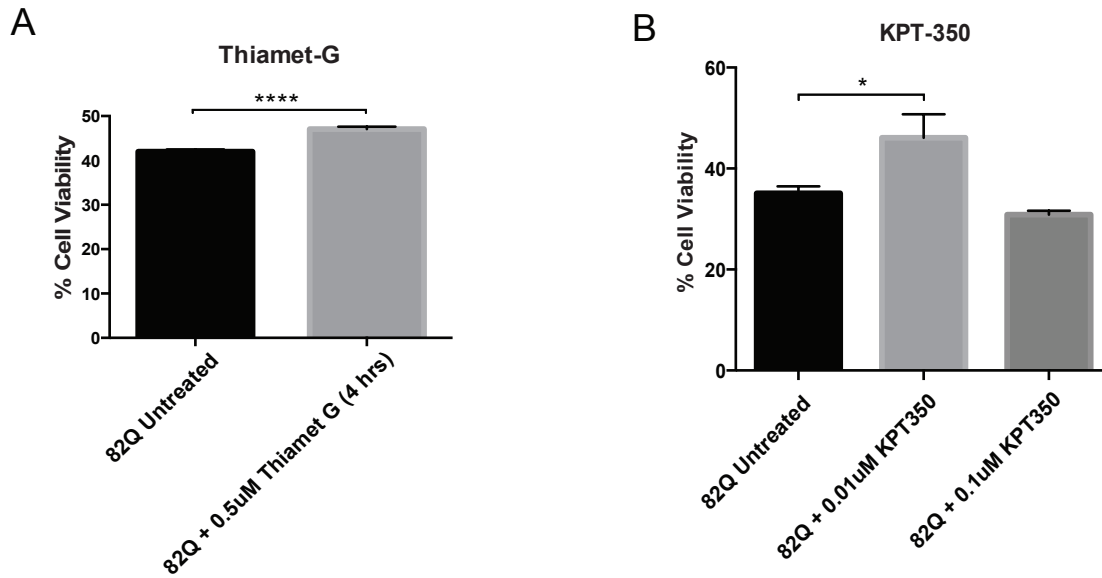


Figure S6 (related to Figure 8). Thiamet-G and KPT-350 Individually Increase Cell Viability in Primary Cortical Neurons Transfected with Full-Length mHTT.

(A) Cell viability is increased in primary cortical neurons transfected with HTT 82Q when treated with 500nM Thiamet G for 4 hours beginning 44 hours after transfection. Experiment represents the average of 4 wells total per condition. (B) Cell viability is increased in primary cortical neurons transfected with HTT 82Q when treated with 0.01uM KPT-350 at the time of transfection for 48 hours. Experiment represents the average of 4 wells. Data (A,B) are presented as mean \pm SEM. * $P < 0.05$ and **** $P < 0.0001$ as analyzed by one-way ANOVA followed by Tukey's post-hoc analysis.

Table S1 (related to Figures 1 and 2). Summary of NUPs and NPC-Associated Proteins Assessed in R6/2 and Q175 Mice
regarding all NUPs and NPC-associated proteins analyzed in R6/2 and Q175 mice, including anatomical location, domain, function, post-translational modification, and antibody used for analysis.

NUP or NPC-Associated	Anatomical Location in	NUP Structures or	NUP Function	Post-translational	Antibody Used
GLE1	Cytoplasmic ring/filaments	Coiled-coils	With cofactor IP6 and Dbp5: stimulates mRNP remodeling and mRNA export, translation	-----	Anti-GLE1 (ab96007)
NUP88	Cytoplasmic ring/filaments	β-propeller and coiled-coils	Together with Nup214, may regulate localization of CRM1	O-GlcNAc	Anti-NUP88 (ab79785)
RanGAP1	Cytoplasmic ring/filaments	Leucine-rich repeats	GTPase activating protein stimulating dissociation of exporter complexes at the NPC	Phosphorylation by CDK1, SUMOylation by SUMO1 for NE targeting	Anti-RanGAP1 (H-180) (sc25630)
RanBP2 (NUP358)	Cytoplasmic ring/filaments	FG repeats	Major component of cytoplasmic filaments, binding site for RanGAP1, also an E3 SUMO-protein ligase	O-GlcNAc, phosphorylation, ubiquitinated by PARK-2, acetylated	Anti-RanBP2 (abn1385)
NUP214	Cytoplasmic ring/filaments	FG and FxFG repeats, β -propeller, coiled-coils	mRNA export by binding Dbp5 (Dickmanns), potentially protein export, together with Nup214, may regulate localization of CRM1	O-GlcNAc	Anti-NUP214 (a300716a)
RanBP17	Cytoplasmic ring/filaments	Belongs to exportin family	Member of importin-beta superfamily of nuclear transport receptors and binds Ran-GTP	-----	Anti-RanBP17 (nbp191029)
ALADIN	Central channel	WD repeats and β -propellers	Selective cargo import; interaction with ferritin heavy-chain (FTH1)	Acetylation, Phosphoprotein (Uniprot)	Anti-Aladin (a304514a)
NUP62	Central channel	Coiled-coils and FG repeats	Associates with importin alpha/β complex during protein import and interacts with NTF2	O-GlcNAc	Anti-NUP62 (sc25523)
NUP54	Central channel	FG repeats	Forms complex with	O-GlcNAc	Anti-NUP54
XPO1 (CRM1/Exportin-1)	Nuclear ring/basket	HEAT repeats	Mediates nuclear protein export for cargoes with a leucine-	Acetylation, Phosphoprotein	Anti-XPO1 (pa513642)
NUP153	Nuclear ring/basket	Zinc fingers	Links TPR to the nuclear basket (Hase and Cordes), high	O-GlcNAc, phosphorylation	Anti-NUP153 (sc292438)
NUP50	Nuclear ring/basket	alpha/ β -domains	Interacts with Nup153 and stimulates importin a/b-dependent import	O-GlcNAc	Anti-NUP50 (pa528452)
TPR	Nuclear ring/basket	heptad repeat / coiled-coil or leucine zipper motifs	Binds to Nup153 at the basket (Xu), forms heterochromatin-exclusion zones (Krull), CRM1-dependent	O-GlcNAc	Anti-TPR (ihc00099)
RCC1	Nuclear ring/basket	RCC1 repeats	Ran guanine-nucleotide exchange factor-reloads GTP at the nuclear face and	Methylation	Anti-RCC1 (hpa027574)
NXF1	Nuclear ring/basket	Leucine-rich repeats and RNP-type RBD	Non-karyopherin transport heterodimer critical for mRNP export	Acetylation, nitration	Anti-NXF1 (ab50609)
NUP98	Central channel and Nuclear basket	FG-repeats, GLFG-repeats, β-sandwich	Binds transporters like importin-β, transportin, and TAP and Rae1, affects transportin-dependent import and promotes CRM1 export	O-GlcNAc	Anti-NUP98 (generously provided by Dr. Michael Matunis)
POM121	Transmembrane	Transmembrane helices and FG-repeats	Anchors the NPC to the NE; recruits Nup62 and Nup358 to the NPC	O-GlcNAc	Anti-POM121 (pa527623)
NUP93	Scaffold	alpha-helical and/or β -propellers	Forms subunit complexes and may serve in anchoring	O-GlcNAc, phosphorylation	Anti-NUP93 (nbp181546)
NUP107	Scaffold	alpha-helical and/or β -propellers	Forms Y-subcomplex with Nup160, an essential structural	O-GlcNAc	Anti-NUP107 (p8530774)
NUP35	Scaffold	alpha-helical and/or β -propellers,RRM, alpha/ β domains	Forms linker nucleoporins with Nup93	O-GlcNAc	Anti-NUP35 (generously provided by Dr. Michael Matunis)

Red = Pathologic

*NUPs and NPC-associated proteins as assessed in R6/2 and

Table S2 (related to Figure 3). Patient Demographics for Postmortem Control, HD, and JHD Brain Tissues. Description of human control, HD, and JHD brain tissues used in this study.

Human Patient Demographics					
FDX	Case Number	Age	Sex/Race	PostMortem Delay	Vonsattel Grade
CTRL	305	60	M/B	12	-
	326	50	M/W	33	-
	354	44	M/W	34	-
	528	31	M/B	26	-
	529*	51	M/W	10	-
	269	29	F/AA	26	-
	394	27	M/W	13	-
	427	23	F/W	40	-
	482	23	F/W	18	-
	518	30	F/W	9	-
	HD	283	51	F/W	22
285		32	M/W	18	4
292		46	F/W	7	4
313		57	M/W	4.5	4
257		44	F/W	5	3
JHD	88	29	F/B	17	4
	105	27	M/W	22	4
	216	23	F/B	14	4
	243	23	F/W	13	3 -- 4
	264	29	F/W	49	4
HD=Huntington's disease					
JHD=Juvenile Huntington's disease					
CTRL= Control					

Table S3 (related to Figure 4). Patient Demographics for Control and HD iPS Cell Lines. Description of human control and HD iPS cell lines used in this study.

Control and HD iPS Cell Lines

iPS Cell Line	Clone	Gender	Diagnosis	CAG repeats	Coriell Catalog ID (fibroblasts)	Reference
CS14iCTR28 (28Q)	n6	F	Clinically normal	28	GM03814	Sareen et al. (2012)
CS03iHD53 (53Q)	n3	M	HD	53	Submitted, pending	HD iPSC Consortium (in press)
CS09iHD109 (109Q)	n1	F	HD	109	ND39258	Mattis et al. (2015)